Georgia Journal of Science

Volume 77 *No. 2 Scholarly Contributions from the Membership and Others*

Article 7

2019

A Brief Review of Modern Uses of Scattering Techniques

Daniel M. Wade
Valdosta State University, dmwade@valdosta.edu

Dereth J. Drake
Valdosta State University, djdrake@valdosta.edu

A BRIEF REVIEW OF MODERN USES OF SCATTERING TECHNIQUES

Daniel M. Wade
Dereth J. Drake
Department of Physics, Astronomy, and Geoscience
Valdosta State University
Valdosta, Georgia, 31698, USA
dmwade@valdosta.edu, djdrake@valdosta.edu

ABSTRACT

Thomson, Rayleigh, Mie, and Raman scattering are commonly used in several disciplines in science and engineering. The techniques involve the scattering of electromagnetic radiation or particles in a sample. This paper provides a brief history for each scattering method, describes the traditional laboratory approach for implementation, and discusses current uses and variations of these four techniques.

Keywords: scattering, Thomson, Rayleigh, Mie, Raman, physics

INTRODUCTION

Scattering is a process in which electromagnetic waves or particles deviate from a straight line due to interference or collision within a medium. For electromagnetic radiation, modification of reflected light from the angle calculated by the law of reflection is included in the definition of scattering (Khanna 2012). For particle-particle collisions, scattering includes collisions between atoms, molecules, electrons, and other particles. Examples include electrons scattered in fluorescent lamps (Bohren and Huffman 2007), certain collisions inside particle accelerators (Bingham and Mandonca 2004), and cosmic rays scattered in Earth's upper atmosphere (Usoskin et al. 2010).

The resulting scattering can be classified into two types: coherent and incoherent. Coherent scattering occurs when particles scatter off multiple objects, and the resulting phase amplitudes add coherently, i.e., all particles act as one in the medium. In contrast, incoherent scattering is when the particles in a medium act independently of one another. For example, when photons undergo coherent scattering from an object, the energy of the scattered photons is typically unidirectional (Prum et al. 2005). For incoherent scattering, the total radiation from the scattering appears to be omnidirectional and tends to be much weaker in amplitude.

There are four common types of scattering techniques:

1. Rayleigh scattering is produced when light is scattered by particles in a medium, without a change in wavelength.
2. Thomson scattering is produced when a charged particle elastically scatters a photon.
3. Mie scattering is a form of scattering of spherical particles based on the Mie solution to Maxwell's equations (Bindsley 1992).
4. Raman scattering is produced when a molecule, excited to higher energy levels, inelastically scatters a photon.

In the following sections of this paper, we describe each of these four techniques, and how they are commonly used today in science and engineering. We also provide a brief history of each technique to allow the reader to better understand the motivation behind the development of each scattering process.

RAYLEIGH SCATTERING

Rayleigh scattering was named after John William Strutt, also known as Lord Rayleigh, who earned a Nobel prize in 1904 for discovering argon and is credited with the discovery of Rayleigh acoustic waves (Lindsay 1970). His technique involves scattering of photons by dielectric particles considerably smaller than the wavelength of the incident radiation, with the criteria that $\alpha << 1$ and $|M|\alpha << 1$, where α is the dimensionless size parameter, given by

$$\alpha = \frac{2\pi r}{\lambda}. \qquad (1)$$

Here M is a constant, r is the spherical radius of the particle, and λ is the relative scattering wavelength. For $\alpha >> 1$, particles much larger than the wavelength of the light are being scattered. This is referred to as geometric scattering. The wavelength of the incident and scattered light remains constant throughout the scattering process (Santra 2017).

One example of Rayleigh scattering is the appearance of our blue sky (Strutt 1870). Blue light is scattered at larger angles than red light. At sunrise or sunset, the path length for sunlight is significantly increased, which causes the light to appear redder than it actually is. On the other hand, during the daytime blue light is typically scattered multiple times before it is observed. The effect of this scattering is that the blue light appears to come from random directions, which is why the sky appears to be blue.

As shown in Figure 1, the laboratory version of this technique involves sending a laser or other electromagnetic source into a sample. Part of the incident light is scattered off the sample and measured by a detector (the black beam in the figure). The signal produced from the scattering, referred to as the feedback, can then be used to measure

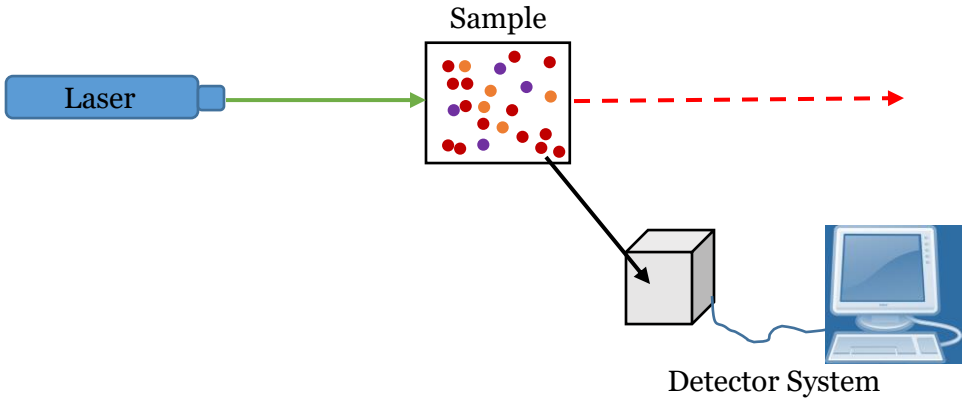

Figure 1. Schematic of a simple Rayleigh scattering experiment. The green solid line represents the incident light and the red dashed line represents the transmitted laser light. The black solid line is the scattered part of the beam that is used for measurements of the sample under investigation by the detector system. Computer image courtesy of http://www.publicdomainfiles.com/show_file.php?id=13938399629439.

specific properties of the sample depending on the angle of the scattered beam and the line shape of the scattered signal.

Rayleigh scattering has two key limitations: (1) it is not species selective as atoms, molecules, and particles scatter at the same wavelength and (2) stray light and surfaces can interfere with the Rayleigh signal. Due to these problems, a corrective measure was developed in the late 1980s and early 1990s known as filtered Rayleigh scattering (FRS) (Forkey 1996). This method has a few conditions (a) that the major species concentrations must be known, as the Rayleigh scattering cross sections differ by species, and (b) proper modeling of the line shape must be employed, especially when at high pressure or with more complicated molecular structures. These conditions allow for Rayleigh scattering to be used in more complex environments and even in a contaminated system.

Rayleigh scattering is typically used nowadays for the characterization of nanoparticles. Nanoparticles are objects that range in diameters from 1 to 100 nm and are most commonly produced in industry by a wet chemical deposition process known as sol-gel (Hench and West 1970). When FRS is used on a solution of nanoparticles, it produces different scattering patterns from the different electron configurations found within each type of molecule and atom that make up the nanoparticles. This allows for researchers to differentiate between the different types of nanoparticles in a composite mixture (Miles et al. 2001). Since nanoparticles are also found in the exhaust from fabrication plants, and the method can be implemented over long distance, FRS can be used to monitor the emission from smoke stacks and exhaust tubes from these facilities (Inaba and Kobyasi 1972; Kobayashi 2012). This technique allows local environmental agencies to monitor the emissions from these stacks to determine what type of atmospheric pollutants are present.

A common variation on this technique is hyper-Rayleigh scattering (HRS). HRS is very similar to other Rayleigh scattering approaches. However, one significant difference is that it induces a second harmonic within the sample being studied, which allows for measurement of the first-order optical hyperpolarizability parameter for organic materials, such as salts, proteins, and octupoles (Stadler et al. 1996; Noordman and van Hulst 1996). Another difference is that HRS looks primarily at the light scattered at 90˚, relative to the incoming wave (Hendrickx et al. 1998), compared to traditional Rayleigh scattering, which looks at light scattered at all angles. In a recent experiment, HRS was used to detect single base-pair mismatches in DNA (Ray 2006; Ray et al. 2009). The experiment used a Q-switch Nd: YAG laser as the light source to incite a second harmonic at 1300 nm. The results showed that HRS is sensitive enough to detect the mismatch without modification to the DNA structure or strands. This indicates that this technique has the sensitivity required to potentially detect pathogens within the human blood stream.

THOMSON SCATTERING

Thomson scattering was named after J. J. Thomson, who first proposed its existence in 1907, and is based on his Nobel prize winning work on the discovery of the mass of the electron (Warner and Hieftje 2002). The method measures the feedback radiated off excited atoms and electrons after interactions with a propagating electromagnetic wave. Ions are typically ignored due to their weak feedback radiation. This method was initially purely theoretical because the technology was not available to perform necessary experiments at the time of Thomson's theory. The first scattering

signal was detected when a powerful radar pulse produced electron scattering in the Earth's ionosphere in 1969 (Evans 1969), nearly 50 years after Thomson first theorized the technique. When laser technology became more readily available in the 1970s, Thomson scattering in the laboratory became possible and led to the modern version that is used today.

Thomson scattering is defined by two key factors: (1) the Debye length λ_D and (2) the differential wave scattering vector σ. The Debye length is a measure of a charge carrier's net electromagnetic effect and how far it persists before quasi-equilibrium is reproduced. The scattering wave vector is the resultant of the radiation of the particles in the medium and is given by

$$\sigma = 1/k\lambda_D \tag{2}$$

where k is the wave number (Glenzer et al. 1999). This equation gives us the ranges for incoherent and coherent scattering if

$$\sigma = \begin{cases} < 0.1 & \text{there is incoherent scattering.} \\ 0.1 \leq \sigma \leq 1.5 & \text{there is coherent scattering.} \\ > 1.5 & \text{there is incoherent scattering.} \end{cases}$$

An issue with this method is that Thomson scattering needs to be calibrated (LeBlanc 2008). This calibration is done by way of Rayleigh scattering, which is performed under similar means of a laser inducing radiation spectrum, i.e., the set-up for Thomson scattering is very similar to that of Rayleigh scattering as shown in Figure 1. The use of the laser for Thomson scattering does not require a total power measurement as Rayleigh does, but instead uses a relative measurement allowing for the scattering to be normalized to the laser signal. As such, there have been experiments where the two techniques have been combined to provide more accuracy when measuring specific parameters within the experimental system (van de Sanden et al. 1992; van der Meiden et al. 2012).

Modern uses of Thomson scattering involve incoherent scattering for temperature and density measurements in electron cyclotron resonance plasmas (ECR) (Bowden et al. 1993). ECRs use permanent magnets or solenoids to generate very strong magnetic fields, which cause the free electrons in a gas to rotate with the same frequency. A microwave source is used in conjunction to the magnets and, once the microwave frequency matches the electron rotation frequency, a plasma will be generated in the device. Testing of ECR high electron density plasmas has led to breakthroughs in nuclear research that were previously impossible in normal plasmas since most plasmas tend to have a low electron density or a high neutral species density. Thomson scattering is employed to monitor the temperature and electron density in the system during any experiment (Sakoda et al. 1991; Beck et al. 2001).

Another use of this type of incoherent scattering techniques is for measurements of Earth's ionosphere. The ionosphere is the layer between 80 and 1000 km above the surface, which contains a large population of ions and electrons. As with ECRs, the technique is used to measure species density, changes in the temperature, and high frequency wave pumping in the ionosphere (Beynon and Williams 1978; Thidé and Lundborg 1986). Most notably these variations occur within the auroras, also known as

the northern and southern lights (Kofman 1992). A more recent use of Thomson scattering is in measuring plasma parameters in manufacturing processing plasmas. Despite the widespread use of processing plasmas (Williams 1997; Boulos 2001; d'Agostino et al. 2005), only recently have comprehensive studies been made into these systems. Thomson scattering is a very common technique since it is in situ and noninvasive, thereby providing decent measurements of the electron temperature, gas temperature, electron density, and neutral gas density (Huang and Hieftje 1982; Mosian et al. 1994; Crintea et al. 2009; Muraoka and Kono 2011).

MIE SCATTERING

In 1908, Gustav Mie, using Maxwell's electromagnetic equations, derived a theory for plasmon resonance absorption for colloid nanoparticles (Bindsley 1992). His theory explained the sharp, particles-size dependent, absorption bands obtained in experiments on gold nanoparticles. He also explained the change in observed wavelength when the size of the colloids was increased from 20 to 1600 nm (Lilienfeld 1991). Mie used a set-up like that of Rayleigh scattering, except he looked at the light scattered off the sample, absorbed by the sample, and the incident radiation reflected back (with $\alpha \sim 1$). This means that Mie's theory could be used to describe Rayleigh scattering, which only looks at the light scattered off the sample.

Mie scattering has previously been used in the biological sciences for studying cytoplasm of living cells (Uličny 1992), casein micelles in milk and other liquid media (Frisvad, et al. 2007), and the orientation of cells in a monoculture cell suspension (Kreid et al. 1973). However, it is most often used for flow visualization in high speed gas flows for qualitative measurements. This is primarily due to its easy implementation, requiring a set-up like Rayleigh, but with the addition of a particulate seed in the gas. The particulate in the gas is known as a tracer and allows for the flow visualization to occur giving valuable data on the flow's structure. This visualization is common in laboratories that work with combustibles and engine development since it allows the flow of different gaseous emissions to be observed leading to improvements in exhaust control (Wendland 1991; Zughyer et al. 2000; Fang et al. 2008). However, one problem with Mie scattering is finding particulate tracers when seeding is necessary. Many tracers that provide a strong signal are highly toxic, such as iodine and nitric oxide (Butler and Williams 1993). The increased danger makes the technique less appealing for university research.

Although a qualitative approach is simple, a quantitative approach to Mie scattering is more difficult and requires improvements in observational equipment. A photomultiplier tube (PMT) is often employed to observe species concentration and concentration fluctuations in turbulent mixes (Long et al. 1981). The PMT is a photoemissive device that amplifies an electronic signal produced by a photocathode exposed to a photon flux. PMTs are used to analyze a single point in the flow-field, which is the area that is occupied by both the flow and its area of influence. This single-point observation technique led to the development of planar Mie scattering (PMS), which uses a two-dimensional array that collects data from illuminated planes in a flow-field, and this allows for concentration field mapping two-dimensional flows (Clemens and Mungal 1991). To perform PMS, a researcher introduces a tracer particulate into the flow and illuminates it with a sheet of light. This creates a bright plane that can be recorded by a CCD camera. The measured light intensity at each pixel on the camera is proportional to the concentration of implanted particles in the flow-field. Thus, PMS gives a two-

dimensional visualization of the flow. This technique is in common use today for studying flow velocimetry with various tracer gases (Lozano et al. 1992; Adrian 2005).

RAMAN SCATTERING

In 1923, Adolf Smekal theorized that photons could be inelastically scattered by molecules that had been excited to higher vibrational or rotational energy levels (Strube 1994). These photons have an energy (E_s) less than the incident ones (E_i). The energy difference is determined by the difference in the vibrational transition energies ($\Delta = E_{vi} - E_{vs}$). This decrease in energy produces a wavelength shift of the scattered light away from the incident wavelength that is dependent on the species present in the gas. Although Smekal first derived the theory, it was C. V. Raman in 1928 who performed the first experiments to verify the theory, and it is from Raman that this scattering technique gets its name.

Raman scattering can be used in situations when molecules have no net dipole moment. This means molecules, when scattered by a photon, will not produce a clean rotational spectrum (Marques 1998). This means that the technique can provide information about molecules that do not have a net polarity. These molecules have a neutral polarity, which helps prevent natural interference in the detected signals, i.e., it depends upon the polarizability of the molecules being studied. The process of Raman scattering provides information about the moment of inertia for the molecule being studied, as well as the molecular structure.

Raman scattering is advantageous in several aspects since (1) it does not require an adjustable laser, just one with a high average power output, (2) several species can be measured simultaneously, and (3) the signal does not suffer from saturation effects as with other scattering techniques. These saturation effects can affect data measurements by interfering with the optical receivers of a spectrometer. Given these advantages over other types of scattering, Raman scattering has shown to be very useful in experimental measurements. In particular, Raman scattering when combined with Thomson and Rayleigh, can provide more detailed measurements of plasma parameters in tokamaks and other nonlinear plasma devices (LeBlanc 2008; Carbone and Nijdam 2015).

Precise Raman scattering measurements are commonly obtained in a laboratory setting when measuring temperatures and major component concentrations of a jet flow (Oschwald and Schik 1999; Cabra et al. 2002). In these experiments, scattering measurements of both rotational and vibrational energies of the molecular species are obtained. The rotational Raman has roughly 10 times the energy of vibrational Raman and can aid in the analysis of multiple species. However, in these experiments several problems have arisen:

1. Both Mie and Rayleigh scattering naturally occur in any Raman scattering experiment. The problem is distinguishing between reactions of Raman, Mie, and Rayleigh scattering signals in the data.
2. Precise quantized measurements are extremely sensitive to stray light and outside pollutants.
3. Raman scattering has an extremely weak signal, about 1000 times weaker than Rayleigh scattering (Marques 1998). This weak signal requires a high output source or an extended averaging time causing it to be highly inefficient.

A common variation of Raman scattering is a technique called Raman excitation plus laser induced fluorescence (RELIEF) (Miles et al. 1989; Miles et al. 2000). The implementation of this technique involves tagging a specified molecule through vibrational excitation and then imaging the tagged molecules after a short time using LIEF. One common usage of this techniques is to simultaneously measure the velocity profiles from a gaseous jet and the density cross section, where the cross section is defined as the difference in density in the area between the particles. RELIEF scattering has the ability not to perturb the flow, and it yields concentration data at all points on the plane (Estruch et al. 2009; Michael et al. 2011).

RELIEF scattering works well in environments where seeding a system is either not possible or unreliable, such as inside a hypersonic jet. This technique also can be used when large scale measurements of a system are necessary, since the density profile can be determined across a large flow area. One problem with RELIEF is that data reduction is required, which entails correcting the intensity variation across the results to eliminate background noise (Brooker et al. 1988). This requires either an extremely controlled environment or time and resources to clean and screen the data for errors.

Another variation of the method is surface enhanced Raman scattering (SERS). This technique involves attaching nanometer sized silver or gold particles to the surface of a sample, and combining them with laser spectroscopy techniques, to produce an enhancement of the Raman scattering signal by a factor of 14–15 (Kneipp 2002; Otto et al. 1992; Xu and Yeung 1997). This enhanced version of the technique allows for the conduction of enzyme immunoassays (Dou et al. 1997), studies of the intercellular distribution of drugs in living cells (Nabiev et al. 1991; Morjani et al. 1993), detection of different neurotransmitters in an aqueous solution (Schulze 1994), and in-depth studies of single molecules that were previously difficult to study, such as the oxygen transport protein hemoglobin (Xu et al. 1999). In a recent study by Fazio et al. (2016), SERS was used to detect phenylalanine, bovine serum albumin, and lysozyme. The technique increased the sensitivity by 10^5, compared to the traditional Raman scattering method. The results indicate that this technique can be used to detect pathology biomarkers in liquid environments when nanoparticles are injected into living cells.

CONCLUDING REMARKS

Thomson, Mie, Rayleigh, and Raman scattering techniques are very similar but there are key differences:

1. Rayleigh scattering is produced when light is elastically scattered by particles in a medium, without a change in wavelength. The particles' diameters must be significantly less than the wavelength of the incident light.
2. Mie scattering is produced when light is elastically scattered by particles in a medium, where the wavelength can change. The particles' diameter is significantly larger than the wavelength of the incident light.
3. Thomson scattering is the elastic scattering of photons by charged particles.
4. Raman scattering is the inelastic scattering of photons by excited molecules.

As discussed in this paper, they all stem from historic experiments and now serve a multitude of functions in modern research and production. The scattering techniques are still being further developed by laboratories and industry for increased efficiency as well as application to new media and environments.

REFERENCES

Adrian, R.J. 2005. Twenty years of particle image velocimetry. Exp. Fluids, 39, 159, doi: 10.1007/s00348-005-0991-7.

Beck, A., D. Hemmers, H. Kempkens, H.B. Schweer, and J. Uhlenbusch. 2001. Comparative measurement of electron density and temperature profiles in low-temperature ECR discharges by a lithium atom beam and Thomson scattering. J. Phys. D Appl. Phys., 33, 360.

Beynon, W.J.G. and P.J.S. Williams. 1978. Incoherent scatter of radio wave from the ionosphere. Rep. Prog. Phys., 41, 910.

Bindslev. H. 1992. On the theory of Thomson scattering and reflectometry in a relativistic magnetized plasma. Optics and Fluid Dynamics (Thesis, University of Oxford).

Bingham, R., J.T. Mandonca, and P.K. Shukla. 2003. Plasma based charged-particle accelerators. Plasma Phys. Control. Fusi., 46, R1.

Bohren, C.F. and D.R. Huffman. 2007. Absorption and Scattering of Light by Small Particles. Wiley.

Boulos, M.I. 1991. Thermal plasma processing. IEEE Trans. Plasma Sci., 19, 1078, doi:10.1109/27.125032.

Bowden, M.D., T. Okamoto, F. Kimura, H. Muta, K. Uchino, and K. Muraoka. 1993. Thomson scattering measurements of electron temperature and density in an electron cyclotron resonance plasma. J. Appl. Phys., 73, 2732.

Brooker, M.H., O. Faurskov Nielsen, and E. Praestgaard. 1988. Assessment of correction procedures for reduction of Raman spectra. J. Raman Spectro. 19, 71.

Butler, A.R. and D.L.H. Williams. 1993. The physiological role of nitric oxide. Chem. Soc. Rev., 22, 233.

Cabra, R., T. Myhrvold, J.Y. Chen, R.W. Dibble, A.N. Karpetis, and R.S. Barlow. 2002. Simultaneous laser Raman-Rayleigh-LIF measurements and numerical modeling results of a lifted turbulent H2/N2 jet flame in a vitiated coflow. Proceed. Combust. Instit., 29, 1881.

Carbone, E. and S. Nijdam. 2015. Thomson scattering on non-equilibrium low density plasmas: Principles, practice, and challenges. Plasma Phys. Control. Fusion 57, 014026, doi:10.1088/0741-3335/57/1/014026.

Chen, S., A. Maksimchuk, and D. Umstadter. 1998. Experimental observation of relativistic nonlinear Thomson scattering. Nature 396, 653.

Clemens, N.T. and M.G. Mungal. 1991. A planar Mie scattering technique for visualizing supersonic mixing flows. Experi. Fluids, 11, 175.

Crintea, D.L., U. Czarnetzki, S. Iordanova, I. Koleva, and D. Luggenhölscher. 2009. Plasma diagnostics by optical emission spectroscopy on argon and comparison with Thomson scattering. J. Phys. D: Appl. Phys., 42, 045208.

d'Agostino, R., P. Favia, C. Oehr, and M.R. Wertheimer. 2005. Low-temperature plasma processing materials: Past, present, and future. Plasma Proces. Polym., 2, 7, doi:10.1002/ppap.200400074.

Dou, X., T. Takama, Y. Yamaguchi, H. Yamamoto, and Y. Ozaka. 1997. Enzyme immunoassay utilizing surface-enhanced Raman scattering of the enzyme reaction product. Anal. Chem., 69, 1492.

Estruch, D., N.J. Lawson, and K.P. Garry. 2009. Application of optical measurement techniques to supersonic and hypersonic aerospace flows. J. Aerosp. Engine., 22, 383.

Evans, J.V. 1969. Theory and practice of ionosphere study by Thomson scatter radar. Proc. of IEEE, 57, 496.

Fang, T., R.E. Coverdill, C.-F. Lee, and R. A. White. 2008. Effects of injection angles on combustion processes using multiple injection strategies in an HSDI diesel engine. Fuel, 87, 3232.

Fazio, B., C. D'Andrea, A. Foti, E. Messina, A. Irrera, M.G. Donato, V. Villari, et al. 2016. SERS detection of biomolecules at physiological pH via aggregation of gold nanorods mediated by optical forces and plasmonic heating. Sci. Reports, 6, 26952, doi:10.1038/srep26952.

Forkey, J.N. 1996. Development and Demonstration of Filtered Rayleigh Scattering (Thesis, Princeton University).

Frisvad, J.R., N.J. Christensen, and H.W Jensen. 2007. Computing the scattering properties of participating media using Lorenz-Mie theory. ACM Trans. Graphics, 26(3), 60.

Glenzer, S.H., W.E. Alley, K.G. Estabrook, J.S. De Groot, M.G. Haines, J.H. Hammer, J.-P. Jadaud, et al. 1999. Thomson scattering from laser plasmas. Phys. Plasmas, 6, 2117.

Hench, L.L. and J.K. West. 1970. The sol-gel process. Chem. Rev., 90, 33.

Hendrickx, E., K. Clays, and A. Persoons. 1998. Hyper-Rayleigh scattering in isotropic solution. Acc. Chem. Res., 31, 675.

Huang, M. and G.M. Hieftje. 1982. A new procedure for determination of electron temperatures and electron configurations by Thomson scattering from analytical plasmas. Spectochi. Acta B: Atom. Spectro., 27, 37.

Inaba, H. and T. Kobayasi. 1972. Laser-Raman radar – laser-Raman scattering methods for remote detection and analysis of atmospheric pollution. Opto-electro., 4, 101.

Khanna, V.K. 2012. Nanosensors: Physical, Chemical, and Biological. Taylor & Francis Group, 103.

Kneipp, K., H. Kneipp, I. Itzkan, R.R. Dasari, and M.S. Feld. 2002. Surface-enhanced Raman scattering and biophysics. J. Phys.: Condens. Matter, 14, R597.

Kobayashi, T. 2012. Overview of Laser Remote Sensing Technology for Industrial Applications, *In* Industrial Applications of Laser Remote Sensing, T. Fukuchi and T. Shiina, eds. Bentham Books, 3–15.

Kofman, W. 1992. Auroral ionospheric and thermospheric measurements using the incoherent scatter technique. Surv. Geophys., 13, 551.

Kreid, D.K., R.J. Goldstein, and M.R. Kammin. 1973. Effect of asphericity of single particle scattering. Appl. Optics, 17, 3152.

LeBlanc, B.P. 2008. Thomson scattering density calibration by Rayleigh and rotational Raman scattering on NSTX. Rev. Sci. Instrum., 79, 10E737, doi:10.1063/1.2956747.

Lilienfeld, P. 1991. Gustav Mie: the person. Appl. Optics, 30, 4696, doi:10.1364/AO.30.004696.

Lindsay, R.B. 1970. Men of Physics Lord Rayleigh - The Man and His Work. Pergamon Press, 227–242.

Long, M.B., B.T. Chu, and R.K. Chang. 1981. Instantaneous two-dimensional gas concentration measurements by light scattering. AIAA J., 19, 1151.

Lozano, A., B. Yip, and R.K. Hanson. 1992. Acetone: a tracer for concentration measurements in gaseous flows by planar laser-induced fluorescence. Exp. Fluids, 13, 369.

Marques, S.J. 1998. Passive Scalar Measurements in Actively Excited Free Shear Flows (Thesis, Virginia Polytechnic Institute and State University).

Michael, J.B., M.R. Edwards, A Dogariu, and R.B. Miles. 2011. Femtosecond laser electronic excitation tagging for quantitative velocity imaging in air. Appl. Optics, 50, 51258.

Miles, R.B., J. Grinstead, R.H. Kohl, and G. Diskin. 2000. The RELIEF flow tagging technique and its application in engine testing facilities and in helium-air mixing studies. Meas. Sci. Technol., 11, 1272.

Miles, R.B., J.J. Connors, E.C. Markovitz, P.J. Howard, and G.J. Roth. 1989. Instantaneous profiles and turbulence statistics of supersonic free shear layers by Raman excitation plus laser-induced electronic fluorescence velocity tagging of oxygen. Experi. Fluids, 8, 17, doi:10.1007/BF00203060.

Miles, R.B., W.R. Lempert, and J.N. Forkey. 2001. Laser Rayleigh scattering. Measurem. Sci. Tech., 12, R33, doi:10.1088/0957-0233/12/5/201.

Morjani, H., J.F. Riou, I.R. Nabiev, F. Lavelle, and M. Manfait. 1993. Molecular and cellular interactions between intoplicine, DNA, and topoisomerase II studied by surface-enhanced Raman scattering spectroscopy. Cancer Res., 53, 4784.

Mosian, M., G. Suave, Z. Zakrzewski, and J. Hubert. 1994. An atmospheric pressure waveguide-fed microwave plasma torch: The TIA design. Plasma Sourc. Sci. Tech., 3, 584, doi:10.1088/0963-0252/3/4/016.

Muraoka, K. and A. Kono. 2011. Laser Thomson scattering for low-temperature plasmas. J. Phys. D: Appl. Phys., 44, 043001.

Nabiev, I.R., H. Morjani, and M. Manfait. 1991. Selective analysis of antitumor drug interaction with living cancer cells as probed by surface-enhanced Raman spectroscopy. Eur. Biophys. J., 19, 311.

Noordman, O.F.J. and N.F. van Hulst. 1996. Time-resolved hyper-Rayleigh scattering: measuring first hyperpolarizabilities of fluorescent molecules. Chem. Phys. Lett., 253, 145, doi:10.1016/0009-2614(96)00218-7.

Oschwald, M. and A. Schik, 1999. Supercritical nitrogen free jet investigated by spontaneous Raman scattering. Experi. Fluids 27, 479.

Otto, A., I. Mrozek, H. Grabhorn, and W. Akemann. 1992. Surface-enhanced Raman scattering. J. Phys.: Condens. Matter, 4, 1143.

Prum, R.O., T. Quinn, and R.H. Torres. 2005. Anatomically diverse butterfly scales all produce structural colours by coherent scattering. J. Exp. Biology, 209, 748, doi:10.1242/jeb.02051.

Ray, P.C. 2006. Diagnostics of single base-mismatch DNA hybridization on gold nanoparticles by using the hyper-Rayleigh scattering technique. Angew. Chem. Int. Ed., 45, 1151, doi:10.1002/anie.200503114.

Ray, P. C., H. Yu, and P. Fu. 2009. Toxicity and environmental risks of nanomaterials: Challenges and future needs. J. Enviro. Sci. Health, 27, 1.

Sakoda, T., S. Momii, K. Uchino, K. Muraoka, M. Bowden, M. Maeda, Y. Manabe, M. Kitagawa, and T. Kimura. 1991. Thomson scattering diagnostics of an ECR processing plasma. Jpn. J. Appl. Phys., 30, L1425.

Santra, B. 2017. In-situ characterization of nanoparticles using Rayleigh scattering. Sci. Rep., 7, 40230, doi:10.1038/srep40230.

Schulze, H.G., M.W. Blades, A.V. Bree, B.G. Gorzalka, L.S. Greek, and R.B. Turner. 1994. Characteristics of backpropagation neural networks employed in the identification of neurotransmitter Raman spectra. Appl. Spectrosc., 48, 50.

Stadler, S., G. Bourhill, and C. Bräuchle. 1996. Problems associated with hyper-Rayleigh scattering as a means to determine the second-order polarizability of organic chromophores. J. Phys. Chem., 100, 6927.

Strube, G. 1994. Raman Scattering, *In* Optical Measurements, F. Mayinger Springer, 215–241.

Strutt, J.W. 1870. On the light from the sky, its polarization, and colour. Philos. Mag., 41, 107.

Thidé, B. and B. Lundborg. 1986. Structure of HF pump in ionospheric modification experiments: linear treatment. Physica Scripta., 33, 475.

Uličny, J. 1992. Lorenz-Mie light scattering in cellular biology. Gen. Physiol. Biophys., 11, 133.

Usoskin, I. G., G.A, Kovaltsov, and I.A. Mironova. 2010. Cosmic ray induced ionization model CRAC: CRII: An extension to the upper atmosphere. J. Geophys. Res. Atmos., 115, D10302(6).

Van de Meiden, H.J., A.R. Lof, M.A. van den Berg, S. Brons, A.J.H. Donné, H.J.N. van Eck, P.M.J. Koelman, et al. 2012. Advanced Thomson scattering system for high-flux linear plasma generator. Rev. Sci. Instrum., 83, 123505, doi:10.1063/1.4768527.

Van de Sanden, M.C.M., G.M. Janssen, J.M. de Regt, D.C. Schram, J.A.M. van der Mullen, and B. van der Sijde. 1992. A combines Thomson-Rayleigh scattering diagnostic using an intensified photodiode array. Rev. Sci. Instrum., 63, 3369.

Warner, K. and G.M. Hieftje.2002. Thomson scattering from analytical plasmas. Spectochi. Acta B: Atom. Spectro., 57, 201.

Wendland, D.W. 1991. Automobile exhaust-system steady-state heat transfer. SAE Technical Paper 931085 (15).

Williams, P. 1997. Plasma Processing of Semiconductors, Springer.

Xu, H., E.J. Bjerneld, M. Käll, and L. Börjesson. 1999. Spectroscopy of single hemoglobin molecules by surface enhanced Raman scattering. Phys. Rev. Lett., 83, 4357.

Xu, X.-H. and E.S. Yeung. 1997. Direct measurement of single-molecule diffusion and photodecomposition in free solution. Science, 275, 1106.

Zughyer, J., F. Zhao, M. Lai, and K. Lee. 2000. A visualization study of liquid fuel distribution and combustion inside a port-injected gasoline engine under different start conditions. SAE Technical Paper 2000010242.